

MyD88 exacerbates immunological pathology in experimental viral fulminant hepatitis*

Jianzhao Deng¹, Qin Ning², Weiming Yan², Xuan Yang¹, Lizhen Zhao¹, Yuzhang Wu³ (✉), Bei Zhang¹ (✉)

¹ Department of Immunology, Medical College of Qingdao University, 308 NingXia Road, Qingdao 266071, China

² Institute of Infectious Disease, Tongji Hospital of Tongji Medical College, Huazhong University of Science and Technology, Wuhan 430030, China

³ Institute of Immunology, Army Medical University, Chongqing 400038, China

Abstract

Objective To explore the role of *MyD88* signaling in MHV-3 virus-mediated fulminant hepatitis.

Methods We evaluated liver lesion status, the expression of multiple pro-inflammatory cytokines and HMGB1, the recruitment of inflammatory ILC3, and mortality in *MyD88*^{-/-} and WT mice.

Results The expression of multiple pro-inflammatory cytokines that recruit inflammatory ILC3 to the liver was severely impaired in *MyD88*^{-/-} mice resulting in reduced liver pathology, viral replication, and mortality post-infection. Additionally, MHV-3 markedly increased the expression of high-mobility group box 1 (HMGB1) in infected hepatocytes/macrophages and induced HMGB1 protein migration from the nucleus to the extracellular milieu, where it activates *MyD88*-dependent inflammation.

Conclusion Our findings indicate that *MyD88* exacerbates immunological pathology in experimental viral fulminant hepatitis.

Key words: *MyD88*; MHV-3; HMGB1; ILC3

Received: 9 January 2019

Revised: 10 March 2019

Accepted: 27 March 2019

Severe viral hepatitis is a disease with a large annual mortality rate. Its main clinical symptoms are massive necrosis of hepatocytes and hepatic encephalopathy. The development of clinically effective interventions has been hindered by insufficient understanding of the immune mechanism of severe viral hepatitis (FH). It was recently found that when BALB/cJ and C57BL/6 mice were infected with mouse hepatitis virus strain-3 (MHV-3), mononuclear/macrophage-specific coagulant and fibrinogen-like protein-2 (FGL2) were up-regulated and the coagulation cascade was activated *in vivo*, resulting in hepatic sinus thrombosis and hepatocyte necrosis. This phenomenon, called virus-induced “procoagulant activity”, is very similar to the clinical manifestations of FH patients [1–3]. Therefore, we used FH animal models infected with MHV-3 to explore the pathogenesis of severe viral hepatitis.

Pattern recognition receptors (PRRs) are key to the early detection of invading pathogens. PRRs are activated

by specific pathogen-associated molecular patterns (PAMPs) that are present in pathogenic microbes or the nucleic acids of viruses or bacteria [4]. Toll-like-receptors (TLRs), the most well-studied group of PRRs, are displayed on the cell surface or within endosomal compartments where they act as molecular sentinels to detect invading microbes [5]. Myeloid differentiation primary response gene 88 (*MyD88*) is a crucial adaptor protein in most *TLR*-dependent inflammatory signaling pathways and activation of *MyD88* leads to the induction of chemokines, inflammatory cytokines, and type I interferons (IFN) through stimulation of NF- κ B, JNK, and p38 MAPK pathway [6]. *MyD88* signaling plays a critical role in immune responses against a wide variety of pathogens including viruses. For example, *MyD88* signaling is not required for clearance of reovirus infection after oral inoculation of mice [7], but *MyD88*-mediated inflammation induces specific antibody production and protects against influenza virus-caused

✉ Correspondence to: Yuzhang Wu. Email: wuyuzhang@tmmu.edu.cn. Bei Zhang. Email: zhangbei124@aliyun.com

* Supported by grants from the National Natural Sciences Foundation of China (No. 81361120400 and 81222023).

© 2019 Huazhong University of Science and Technology

mortality [8-9]. Conversely, *MyD88*^{-/-} mice infected with lymphocytic choriomeningitis virus (LCMV), vesicular stomatitis virus (VSV), respiratory syncytial virus (RSV), and a recombinant mouse-adapted SARS-CoV virus (rMA15) have more severe pathology than that of the WT [10-13]. Nevertheless, the role of *MyD88* signaling in MHV-3 virus-mediated pathogenesis has not yet been investigated.

Damage-associated molecular patterns (DAMPs), which have the capacity to activate TLRs, are substances produced by damaged or dead cells that initiate inflammatory responses in a paracrine manner [14]. High-mobility group box 1 (HMGB1), a non-histone chromatin-associated nuclear protein, is a classic DAMP, which is highly expressed in most eukaryotic cells. Within the nucleus, HMGB1 acts as an architectural protein that binds to DNA and promotes the assembly of nucleoprotein complexes, thereby facilitating maintenance of genome stability [15-16]. Conversely, exogenous stimulation, including pathogen infection, can lead to cytoplasmic translocation of HMGB1 and its subsequent release into the extracellular milieu [17]. Cytoplasmic translocation and release of HMGB1 by virus-infected cells has been reported following infection with Dengue virus, HIV, West Nile virus (WNV), herpes simplex virus type 2 (HSV-2), hepatitis C virus (HCV), and porcine reproductive and respiratory syndrome virus (PRRSV) [18]. HMGB1 concentrations were significantly higher in patients infected with WNV and HCV [19-20]. Additionally, HMGB1 also supports influenza virus growth by enhancing the activity of viral polymerases [21]. However, whether HMGB1 participates in the pathogenesis of MHV-3 as a host-derived molecular factor remains to be determined.

In a mouse model of FH caused by MHV-3 infection, we found that MHV-3 markedly increased the expression of HMGB1 in infected cells and induced the migration of HMGB1 protein from the nucleus to the extracellular milieu, where it activated *MyD88*-dependent inflammation. Therefore, mice deficient in *MyD88* (*MyD88*^{-/-}) are resistant to MHV-3-mediated FH because of reduced expression of multiple pro-inflammatory cytokines and limited recruitment of pro-inflammatory NKp46⁺Lin⁻Thy1.2⁺Royt⁺ ILC3 to the liver compared to WT littermates. This work suggests that *MyD88* may play an essential role in the pathogenesis of viral FH.

Materials and methods

Mice

C57BL/6 background *MyD88*-deficient (*MyD88*^{-/-}, #009088), *IL-1RI*^{-/-} (#003245), *TNF-α*^{-/-} (#005540), *Rag-1*^{-/-} (#002216) and wild type (WT) mice were imported from the Jackson Laboratory (Bar Harbor, Maine, USA).

Trif^{-/-} C57BL/6 background mice were purchased from *Oriental BioService* (OBS) in Kyoto, Japan [22]. *Fgl2*^{-/-} mice were kindly provided by Prof. Gary Levy (Multi Organ Transplant Program, University Health Network, University of Toronto, Toronto, Canada). Mice were maintained in the animal facility, fed with standard laboratory chow diet and water, and housed in the animal colony at the animal center of Army Medical University. Mice of approximately 12 weeks of age were used for these experiments.

Cells

Raw264.7 cells were provided by the Cell Institute of the Chinese Academy of Sciences (Shanghai, China). GM-CSF-induced BMDMs and peritoneal exudative macrophages (PEMs) were prepared. Cells were cultured in 6-well plates and propagated in DMEM supplemented with 10% FBS, 100 μg/mL streptomycin, and 100 U/mL penicillin.

Virus and infection

MHV-3 viruses were amplified in murine 17CL1 cells to a concentration of 1×10⁷ plaque forming unit (PFU)/mL. Supernatants containing the virus were stored at -80 °C until use. Raw264.7 cells were infected with MHV-3 (multiplicity of infection, MOI = 1) in vitro and mice were injected intraperitoneally (i.p.) with 100 PFU of MHV-3. The virus titers in liver were determined by plaque assay.

Tissue morphology detection and immunohistochemistry

Paraffin-embedded liver tissue blocks were cut into 4 μm slices. Endogenous peroxidase activity was blocked with 2.0% H₂O₂ for 20 min. The slides were then immersed in citrate buffer (pH 6.0) for 10 min at 120 °C. Sections were then incubated overnight at 4 °C with anti-mouse FGL2 (Santa Cruz, USA, 1:100, mouse), anti-Fibrinogen (Abcam, Cambridge, England, 1:1000, Rabbit), anti-HMGB1 (Santa Cruz, USA, 1:50, mouse), anti-TNF-α (Cell Signaling Technology (CST), 1:100, rabbit), anti-IL-6 (Santa Cruz, 1:200, mouse), anti-IFN-γ (Santa Cruz, 1:200, rat), and anti-pro-IL-1β (CST, 1:100, mouse). After washing, the sections were incubated with the corresponding secondary antibodies for 2 h at room temperature. A Vectastain ABC kit (Vector Laboratories, San Diego, USA) was used to create avidin-biotin complexes, which were then visualized with a DAB kit (K3465, DAKO), where brown coloration of tissues represented positive expression. Histopathological analysis of liver was performed by hematoxylin and eosin (H&E). Cellular apoptosis was detected by TUNEL staining (Roche, Berlin, Germany) according to the manufacturer's instructions.

Immunofluorescence staining

Paraffin-embedded tissue blocks were cut into 5 mm slices, which were mounted on polylysine-charged glass slides. Endogenous peroxidase activity was blocked with 2.0% H₂O₂ for 25 min. The glass slides were then placed in citrate buffer (pH 6.0) for 10 min at 120 °C. Sections were then incubated overnight at 4 °C with anti-HMGB1 (eBioscience). After washing, sections were further incubated with the corresponding fluorescent secondary antibodies for an additional 1 h. Finally, the sections were incubated with 1 µg/mL DAPI (Sigma, St. Louis, MO, USA) for 10 min to stain the nuclei. Sections incubated with isotype control antibodies were used as negative controls. The results were visualized using fluorescence microscopy (Nikon, Tokyo, Japan).

Real-time quantitative RT-PCR

TRIzol reagent (Invitrogen, NY, USA) was used to extract total RNA from cultured cells or liver tissues according to the manufacturer's instructions. Reverse transcription was used to synthesize cDNA using a PrimeScript RT-PCR Kit (Takara, Dalian, China). The expression of mRNA encoding for proinflammatory cytokines (including *TNF-α*, *IL-6*, *IFN-γ*, *fgl2*, *proIL-1β*, *HMGB1*) was quantified by real-time quantitative PCR with the SYBR Premix ExTaq kit (Takara, Kyoto, Japan) and normalized to β-actin expression. The primer sequences are shown in Table 1. Relative mRNA expression was calculated and compared by the 2^{-ΔΔC_t} method.

ELISA and western-blotting

Serum FGL2, IL-17, TNF-α, IL-1β, and HMGB1 levels were measured by ELISA. The expression of HMGB1, FGL2, TNF-α, and IL-6 in MHV-3 infected livers was detected by western-blotting.

Flow cytometry

Liver infiltration by GR-1^{high}CD45⁺ neutrophils, CD11b⁺/F4/80⁺ monocytes/macrophages, and NKp46⁺ Lin⁻Thy1.2⁺Royt⁺ ILC3, and the secretion of TNF-α, IL-6, and proIL-1β from PEMs isolated from virus-infected mice at 24 h were detected by flow cytometry (FACSARIA

cytometer, BD, Franklin Lakes, NJ, USA). Dead cells were excluded by staining with a LIVE/DEATH® Fixable Near-IR Dead Cell Stain Kit (Life technologies, Eugene, Oregon, USA). In total, 10,000 live cells were analyzed. All the FACS data were analyzed using CellQuest Pro software. These antibodies were purchased from eBioscience.

Statistical analysis

Statistical analysis of the data was performed using GraphPad Prism 6.0. An unpaired Student's *t*-test (two-tailed) was used to compare two groups when the data met the assumptions of the *t*-test. Survival curves were generated using the log-rank test. *P* < 0.05 was considered statistically significant.

Results

Reduced liver tissue lesions and mortality in *MyD88*^{-/-} mice post MHV-3 infection

To assess the contributions of innate and adaptive immune responses in MHV-3-induced FH, age matched C57BL/6 (WT, *n* = 10), congenic *Rag-1*^{-/-} (*n* = 6), *MyD88*^{-/-} (*n* = 11) and *Trif*^{-/-} (*n* = 5) mice were infected with MHV-3 (100 PFU) via *i.p.* injection and monitored for virus-induced mortality. Surprisingly, we found that all the WT, *Rag-1*^{-/-} and *Trif*^{-/-} mice died within 8 days of infection, whereas over 72.7% (8/11) of the *MyD88*^{-/-} group were still alive after 20 days (*P* = <0.0001, Fig. 1a). Hematoxylin and eosin (H&E) staining showed severe necrosis with sparse polymorphonuclear leucocyte infiltration in the livers of WT mice at both 48 h and 72 h post MHV-3 infection. In contrast, the morphology of *MyD88*^{-/-} livers was mostly normal after 48 h, and the area of necrosis was also dramatically smaller at 72 h (Fig. 1b). Additionally, fewer cells were found to be apoptotic in MHV-3 infected *MyD88*^{-/-} livers 72 h postinfection (Fig. 1c). The expression of biliary glycoprotein-1 (Bgp1), the receptor for MHV-3 [23], appeared to be significantly lower in viral infected *MyD88*^{-/-} livers than in the WT controls (Fig. 1d), supporting the plaque assay showing limited virus entry and amplification in *MyD88*^{-/-} livers 72 h postinfection (Fig. 1e). These findings indicate that the absence of *MyD88* but not *Trif* significantly protects

Table 1 Primer sequences for RT-qPCR

Drug	Forward-primers	Reverse-primers
TNF-α	CACGCTCTTCTGTCTACTGAAC	ATCTGAGTGTGAGGGTCTGG
IL-6	TAGTCCTTCCCTACCCCAATTTCC	TTGGTCCTTAGCCACTCCTTC
FGL2	TGGACAACAAAGTGGCAAATCT	TGGAACACTTGCCATCCAAA
IFN-γ	TCAAGTGGCATAGATGTGGAAG	CGCTTATGTTGTTGCTGATGG
pro-IL-1β	GACAGTGATGAGAATGACCTGTTC	CCTGACCACTGTTGTTTCCC
HMGB1	GATTATCGTTCTCTTAAAGTGCCAG	TATCATCCAGGACTCATGTTTCAGTA
β-actin	ATATCGCTGCGCTGGTCGTC	AGGATGGCGTGAGGGAGAGC

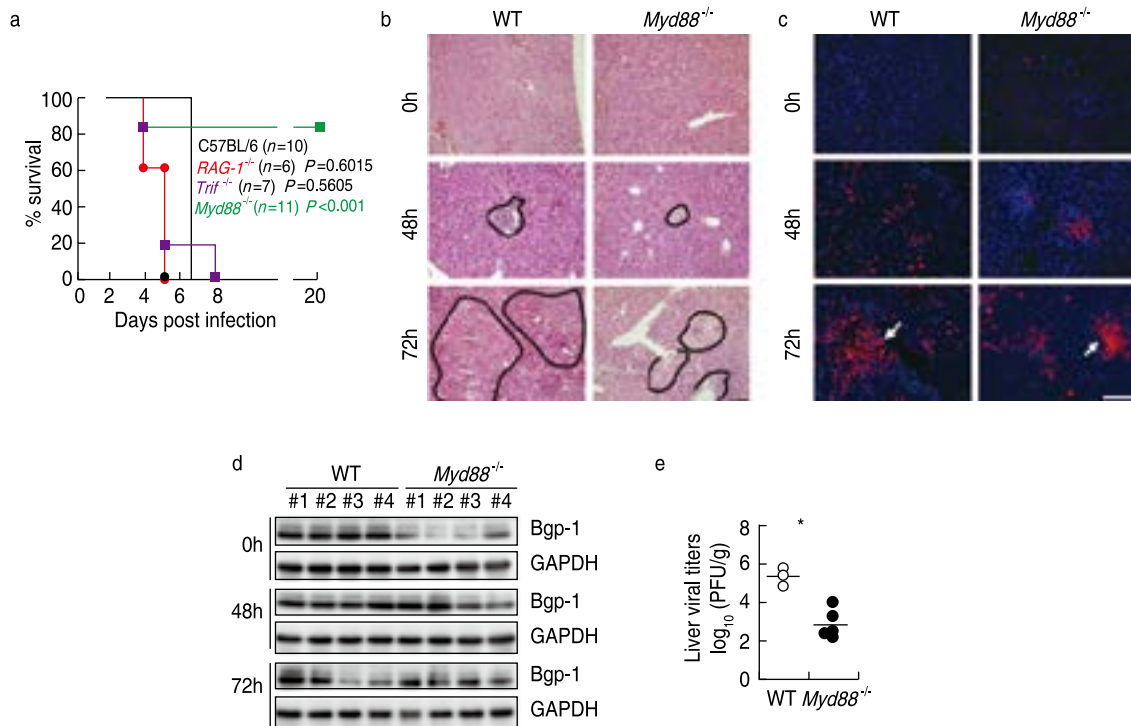


Fig. 1 *MyD88* deficiency attenuates MHV-3-induced hepatitis. Age matched C57BL/6 (WT) and congenic *MyD88*^{-/-} mice were infected with MHV-3 (100 PFU), (a) the survival rate was monitored for a total of 20 days. One representative of three experiments with similar results is shown. **P* < 0.05. Liver tissues were isolated from virus infected WT and congenic *MyD88*^{-/-} mice at different time points; (b) The morphology was analyzed by H&E staining; (c) Cells undergoing apoptosis was analyzed by TUNEL staining. Scale bar = 20 μm; (d) The expression of Bgp1 in livers at 24 h and 72 h post-infection was analyzed by western-blotting. Four representative samples *per* group are shown; (e) The virus titers in livers at 72h post-infection were analyzed by plaque assay, and results were compared by statistical analysis. **P* < 0.05

against MHV-3-induced morbidity and mortality, while adaptive immunity (*Rag-1* deficiency) does not play a major role in the pathogenesis.

MHV-3 fails to induce the production of FGL2 and other pro-inflammatory cytokines in *MyD88*^{-/-} mice

FGL2 plays an essential role in inducing hepatocellular necrosis following MHV-3 infection [2], we therefore examined *fgl2* expression in liver tissues isolated from MHV-3 infected *MyD88*^{-/-} mice. Quantitative RT-PCR (qRT-PCR) showed that *fgl2* mRNA transcription in the liver was induced by MHV-3, and that its expression was dramatically reduced in *MyD88*^{-/-} livers (Fig. 2a). The reduction in FGL2 protein levels in virus-infected *MyD88*^{-/-} livers was also confirmed by western-blot (Fig. 2b), and the FGL2 serum concentration in *MyD88*^{-/-} mice was substantially lower 72 h postinfection (Fig. 2c). Therefore, *MyD88*^{-/-} mice responded with limited fibrinogen formation, leading to reduced liver coagulation and necrosis (Fig. 2d). Moreover, the *Fgl2*^{-/-} mice were completely resistant to MHV-3-mediated mortality (Fig. 2e). These results suggest that the attenuation of viral FH

by *MyD88* deficiency could be the result of suppressed FGL2 production.

Pathologic proinflammatory cytokines, including TNF-α, IL-1β, and C5a, can promote FGL2 expression and worsen the pathogenesis of MHV-3-mediated FH [24-26]. To clarify the molecular mechanism that is responsible for *MyD88* signaling-mediated FGL2 upregulation, liver tissues were isolated from MHV-3-infected *MyD88*^{-/-} mice and their control littermates 72 h post MHV-3 infection. The expression of some proinflammatory cytokines including *Ifn-γ*, *Tnf-α*, *proIl-1β*, and *Il-6* was measured by qRT-PCR. Interestingly, the concentrations of these cytokines were significantly reduced in *MyD88*^{-/-} mice compared to their viral-infected WT littermates (Fig. 3a). These results were also confirmed at the protein level by western-blot (Fig. 3b) and immunohistochemistry (Fig 3c). Finally, we showed that both *Tnf-α*^{-/-} and *IL-1R*^{-/-} mice are phenocopied *MyD88*^{-/-} mice and are resistant to MHV-3-mediated mortality (Fig. 3d). These results indicate that *MyD88* is required for the induction of *fgl2* and other proinflammatory cytokines in response to MHV-3 infection.

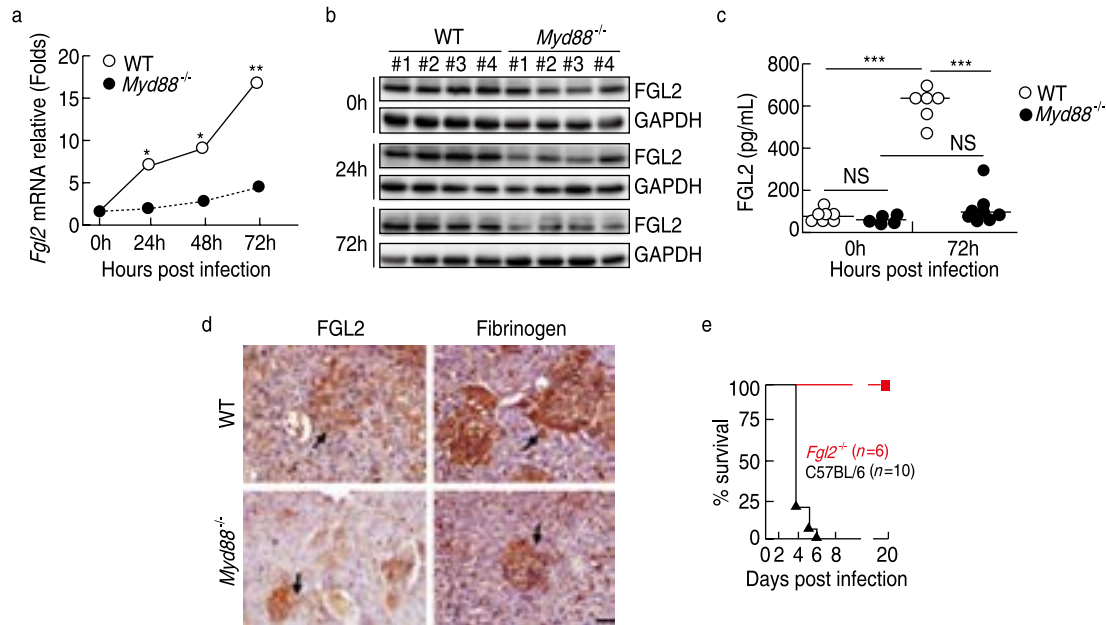


Fig. 2 Reducing FGL2 expression and FB deposition in *MyD88*^{-/-} livers post MHV-3 infection. *MyD88*^{-/-} mice and their C57BL/6 WT littermates were infected with MHV-3 (100 PFU). (a) Liver *fgl2* mRNA transcription was detected by quantitative RT-PCR at different time points; (b) Liver FGL2 protein expression at 24 h and 72 h post infection was detected by Western-blot, *n* = 4 per group; (c) Serum accumulation of FGL2 at 72h of infection was measured by ELISA; (d) Liver fibrinogen deposition was detected by immunohistochemistry; (e) Age matched C57BL/6 (WT) and congenic *Fgl2*^{-/-} mice were infected with MHV-3 (100 PFU), the survival rate was monitored for a total of 20 days. One representative of three experiments with similar results is shown. **P* < 0.05, *n* = 5 per group

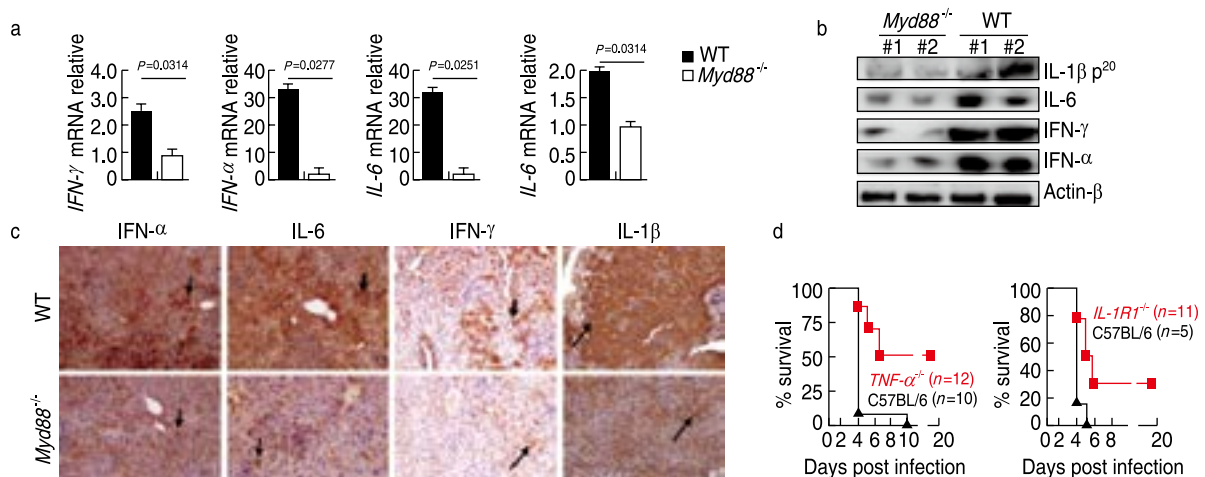


Fig. 3 Reducing proinflammatory cytokine secretion in *MyD88*^{-/-} livers post MHV-3 infection. *MyD88*^{-/-} mice and their C57BL/6 WT littermates were infected with MHV-3 (100 PFU). (a) The transcription of pathologic proinflammatory cytokines, including *TNF-α*, *proIL-1β*, and *IL-6* in MHV-3-infected liver tissues at 72 h was detected by quantitative RT-PCR; (b) The expression of pathologic proinflammatory cytokines in MHV-3-infected liver tissues at 72 h was analyzed by western-blot; (c) The expression of pathologic proinflammatory cytokines in MHV-3-infected liver tissues at 72 h was analyzed by immunohistochemistry; (d) Age matched C57BL/6 (WT) and congenic *IL-1R1*^{-/-}, *TNF-α*^{-/-} mice were infected with MHV-3 (100 PFU), the survival rate was monitored for a total of 20 days. One representative of three experiments with similar results is shown. **P* < 0.05, *n* = 5 per group

The recruitment of pro-inflammatory NKp46⁺ Lin⁺Thy1.2⁺Royt⁺ group 3 innate lymphoid cells was severely impaired in *MyD88*^{-/-} livers post

MHV-3 infection

Monocytes/macrophages and neutrophils are known to be crucial during viral FH due to these cells capacity

to produce pro-inflammatory cytokines, including FGL2 [26]. We determined whether liver infiltration of these cells was affected by *MyD88* signaling during viral FH. Liver infiltration by both CD11b⁺/F4/80⁺ monocytes/macrophages and Gr-1^{high}CD45⁺ neutrophils was detected by flow cytometry in mice infected with MHV-3 (Fig. 4a). However, the difference between these two groups was not statistically significant (Fig. 4b), suggesting that liver infiltration by monocytes/macrophages and neutrophils was not affected by *MyD88* signaling.

Innate lymphoid cells (ILCs) have recently been discovered to play an important role in protective immunity against microbes like intracellular parasites, bacteria, fungi, and parasitic worms [27–28]. Flow cytometry showed that in liver-tissue samples 24 h and 48 h postinfection, infiltration by ILCs (Lin-Thy1.2⁺) was significantly higher in the WT than in their *MyD88*^{-/-} littermates (Fig. 4c and 4d). Additionally, statistical analysis showed that NKp46⁺ Lin⁺ Thy1.2⁺ Royt⁺ ILC3s were severely impaired in MHV-3-infected *MyD88*^{-/-} liver

tissues (Fig. 4d). Furthermore, these ILC3 have the ability to produce proinflammatory mediators, like TNF- α , proIL-1 β , and IL-17 (Fig. 4e). These results suggest that attenuation of viral FH by *MyD88* deficiency could be at least partly due to limited proinflammatory NKp46⁺ Lin⁺ Thy1.2⁺ Royt⁺ ILC3 infiltration into the liver.

Reduced secretion of HMGB1 in *MyD88*^{-/-} mice post MHV-3 infection

HMGB1 is one of the canonical DAMPs that can be either passively released from necrotic/damaged cells, or can be secreted by activated innate immune cells. In addition to its nuclear role, extracellular HMGB1 triggers proinflammatory responses through *MyD88* signaling [29–30]. Thus, we decided to investigate the role of HMGB1 in the Raw264.7 macrophage cells infected with MHV-3 (MOI = 1) by immunofluorescent confocal microscopy showed that HMGB1 localized to the nucleus of mock-infected Raw264.7 cells but was distributed in both the nucleus

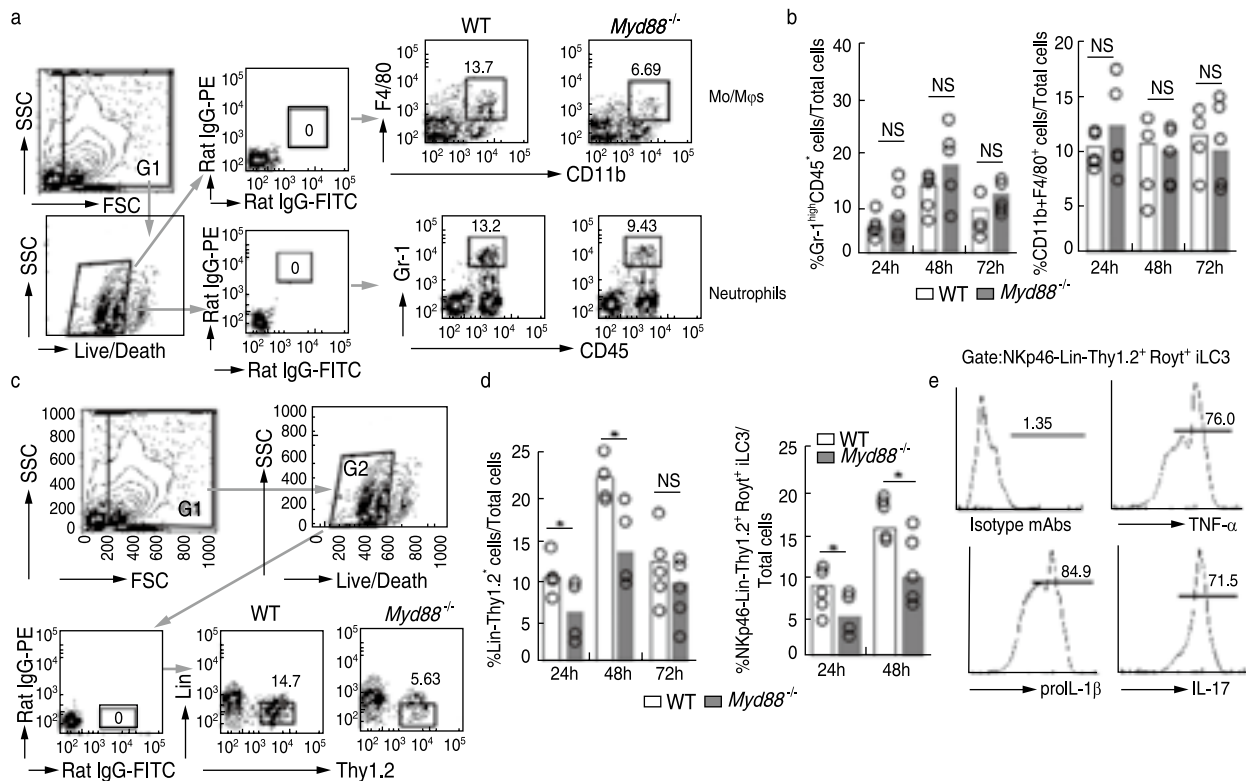


Fig. 4 *MyD88* deficiency prevents the recruitment of proinflammatory NKp46-Lin-Thy1.2⁺ Royt⁺ ILC3 into livers. Age matched C57BL/6 (WT) and *MyD88*^{-/-} mice were infected with MHV-3 (100 PFU), cells were isolated from virus infected livers. (a) Liver recruitment of CD11b⁺/F4/80⁺ monocytes/macrophages, Gr-1^{high}CD45⁺ neutrophils of infection was measured by flow cytometry. Number indicates the percentage of positive cells in the gate. One representative sample from five mice *per* group is showed; (b) Statistical analysis of liver infiltration of CD11b⁺/F4/80⁺ monocytes /macrophages, Gr-1^{high}CD45⁺ neutrophils at 24 h, 48 h and 72 h; (c) Liver infiltration of Lin-Thy1.2⁺ ILCs of MHV-3 infection was detected by flow cytometry; (d) Statistical analysis of liver infiltration of Lin-Thy1.2⁺ ILCs and NKp46⁺ Lin⁺ Thy1.2⁺ Royt⁺ ILC3 of MHV-3 infection; (e) The secretion of IL-17, TNF- α and IL-1 β from NKp46⁺ Lin⁺ Thy1.2⁺ Royt⁺ ILC3 was analyzed by flow cytometry. One representative of three experiments with similar results is shown. **P* < 0.05, *n* = 5 *per* group

and cytoplasm of their MHV-3-infected counterparts (Fig. 5a). Furthermore, a time-dependent increase in HMGB1 supernatant concentration was seen over 72 h of infection (Fig. 5b). Immunohistochemistry showed that HMGB1 protein was localized in nucleus of hepatocytes/macrophages of normal liver tissues, whereas it was mostly found within the cytoplasm of MHV-3-infected hepatocytes, especially in necrotic liver tissue (Fig. 5c). HMGB1 is secreted by damaged/necrotic hepatocytes and *MyD88* deficiency protects the liver from necrosis during MHV-3 infection, suggesting that *MyD88* signaling controls HMGB1 expression. To investigate this possibility, the serum concentration of HMGB1 in MHV-3 infected mice was measured by ELISA, and HMGB1 levels were found to be severely reduced in virus-infected *MyD88*^{-/-} mice compared to their WT littermates (Fig. 5d). Moreover, MHV-3 infected *MyD88*^{-/-} liver tissues also exhibited reduced HMGB1 protein (Fig. 5e). This combination indicates that the virus triggers HMGB1 expression in the infected cells and induces HMGB1 migration from the nucleus to the cytoplasm. *MyD88*^{-/-} mice are protected from MHV-3 infection via reduced HMGB1 concentration in infected liver tissues.

Discussion

Viral fulminant hepatitis (FH) has become a major public health concern. However, insufficient understanding of the immune mechanisms at play in severe viral hepatitis has largely hampered the development of clinically effective interventions. When BALB/cj and C57BL/6 mice were infected with MHV-3, their mononuclear/macrophage cells were activated, resulting in a significant increase in proinflammatory mediators, eventually leading to hepatic sinus thrombosis and hepatocyte necrosis [1-3]. These syndromes are very similar to the clinical manifestations in FH patients. Therefore, the mouse FH model can improve our understanding of the pathogenesis of the disease. In this study, we report that mice deficient in *MyD88* are resistant to MHV-3-mediated FH due to limited recruitment of proinflammatory NKp46⁺ Lin⁻ Thy1.2⁻ Royt⁺ ILC3 to the liver, as well as reduced expression of multiple proinflammatory cytokines like TNF- α , IFN- γ , IL-6 and FGL2, thus limiting liver pathology and prolonging survival post-infection. MHV-3 also triggers the expression of HMGB1 in infected hepatocytes/

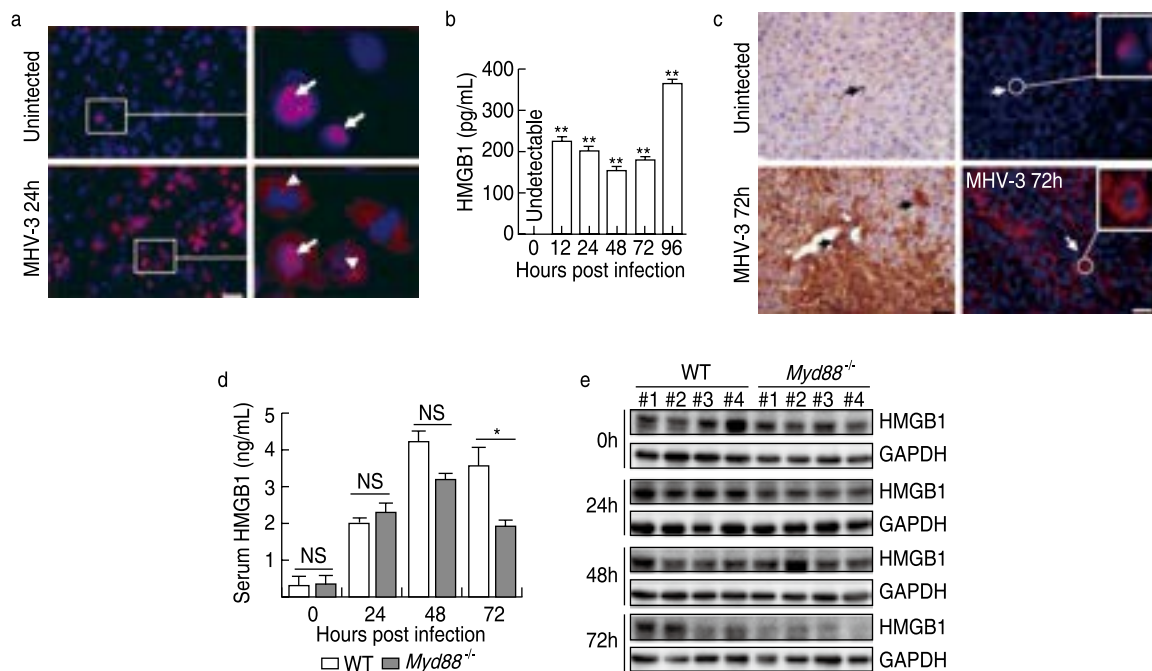


Fig. 5 *MyD88* deficiency reduced the secretion of HMGB1. The macrophage cell line, Raw264.7 cells, were infected with MHV-3-infected (MOI = 1). (a) HMGB1 localization before and after 24 h of infection was monitored by immunofluorescent confocal microscopy; (b) The accumulation of HMGB1 in the supernatants was detected by ELISA; (c) The expression of HMGB1 protein in normal and MHV-3-infected liver tissues was detected by immunohistochemistry; (d) Serum concentration of HMGB1 in *MyD88*^{-/-} and WT mice was detected by ELISA, $n = 5$ per group, * $P < 0.05$; (e) Liver concentration of HMGB1 in *MyD88*^{-/-} and WT mice was detected by western-blot, $n = 4$ per group, * $P < 0.05$

macrophages and induces HMGB1 translocation from the nucleus to the cytoplasm and extracellular milieu, where HMGB1 induces *MyD88* dependent proinflammatory cytokine secretion. These results demonstrate that the *MyD88* is part of the essential signaling pathway in controlling inflammation in the viral FH.

FGL2 plays a key role in fulminant hepatitis and host death caused by MHV-3 infection. By blocking the expression of FGL2, sinus fibrin deposition and hepatocyte necrosis can be effectively prevented, thereby reducing the mortality of infected mice [31–32]. Previous studies have shown that pro-inflammatory cytokines, including IL-1 β , TNF- α , IFN- γ and complement C5a, can aggravate MHV-3-induced FH by promoting FGL2 expression and increasing liver fibrinogen accumulation [24–26]. However, the mechanism by which MHV-3 induces an inflammatory response is unclear. *MyD88* is a key adaptor protein for most TLR-dependent inflammatory signaling pathways as well as the *IL-18R1*, *IL-1R1*, and *IFN- γ R1* signaling cascades [6]. Although *MyD88*-mediated proinflammatory signaling has been implicated in the protection from numerous bacterial and parasitic infections, few *in vivo* studies have found that *MyD88* is protective against viral diseases. Here, we showed that WT C57BL/6 mice are susceptible to lethal MHV-3 infection by a *MyD88*-dependent induction of proinflammatory mediators, and the recruitment of NKp46⁺Lin⁻Thy1.2⁻Royt⁺ ILC3 to the liver. Conversely, *MyD88*^{-/-} mice are resistant to MHV-3-mediated hepatitis and mortality by preventing proinflammatory cytokine and ILC3 accumulation and thus attenuating FGL2 expression (Fig. 1, Fig. 2 and Fig. 3). Our results differ from previous virological studies, which have shown that *MyD88*^{-/-} mice infected with VSV, RSV, LCMV or rMA15 viruses have more severe diseases [33–34]. These results also differ from those seen in MHV-68 viral infections, where *MyD88*-dependent induction of type-I IFN is crucial to control viral replication [35]. These unexpected results imply that *MyD88* has dual effects on the immune system and that the proper balance of its signaling is essential for host protection against various invading viruses as well as prevention of potential collateral damage to the host.

Innate immune cells (ILCs) are lineage negative (Lin⁻) lymphocytes generated by the post fetal liver, which are divided in three major subgroups according to their functional and phenotypic characteristics. These include group 1 (which produces IFN- γ and IL-17), group 2 (which produces IL-4 and IL-5) and group 3 (which produces IL-22 and IL-17) ILCs [36–37]. Previous work has shown that ILC3s in lymphoid tissues from SIV-infected macaques can be induced to undergo apoptosis by microbial products through the TLR2 or TLR4 pathway [38]. Moreover, ILCs depletion resulted in the loss of airway epithelial integrity, diminished lung

function and impaired airway remodeling after influenza virus infection [39]. Here, we showed that *MyD88*^{-/-} mice are protected from lethal MHV-3 infection by lack of recruitment of NKp46⁺Lin⁻Thy1.2⁻Royt⁺ ILC3 to the liver, which may contribute to the pathogenesis of MHV-3-induced FH as these cells have the capacity to produce proinflammatory mediators including TNF- α , IL-17 and FGL2 (Fig. 4c, 4d and 4e). However, we showed that liver recruitment of neither CD11b⁺F4/80⁺ monocytes/macrophages, nor Gr-1^{high}CD45⁺ neutrophils were impaired by *MyD88* signaling (Fig. 4a and 4b), although these cell types have the capacity to promote liver damage by inducing the expression of proinflammatory mediators and boosting viral replication [40–41]. The combination of these results suggests that hepatic infiltration of NKp46⁺Lin⁻Thy1.2⁻Royt⁺ ILC3 actively participates in MHV-3-induced hepatitis.

It is critical to identify and characterize “non-PAMP” host-derived molecular patterns that can activate *Myd88*. HMGB1 protein is a highly conserved nuclear protein that participates in DNA organization and the regulation of transcription [15–16] and can be released passively by necrotic and damaged somatic cells into the extracellular milieu [15–16]. HMGB1 activates macrophages/monocytes and endothelial cells to express pro-inflammatory cytokines, chemokines and adhesion molecules by interacting with its receptors, including RAGE, as well as TLR2 and TLR4, in the extracellular space [42]. The contributions of HMGB1 to the pathogenesis of viral infectious diseases have been well described, for examples, both RNA virus (WNV, Dengue virus, and HIV-1) and DNA virus (HSV-2) infections have been shown to result in the secretion of HMGB1 through apoptosis and/or necrosis [43–44], and the elevation of HMGB1 levels in the plasma of HCV patients with chronic hepatitis, liver cirrhosis, and HCC likely is attributable to the cytopathic effects of HCV infection [20]. We found that MHV-3 induces the migration of HMGB1 from the nucleus to the cytoplasm and its accumulation in the supernatants of infected Raw264.7 cells. Moreover, enhanced HMGB1 protein serum concentration was also seen in MHV-3 infected mice (Fig. 5). Therefore, HMGB1 may participate in MHV-3-mediated pathogenesis by acting alone or in combination with other proinflammatory cytokines.

In summary, our study shows that *MyD88*-dependent proinflammatory cytokine production plays a double-edged role in the host immune system. Hepatotropic viral infections, like MHV-3 infections in mice, can induce excessive inflammation of the liver and cause life-threatening viral FH. These results suggest a novel strategy, which would involve modulation of the *MyD88* signaling pathway, in combination with blocking other inflammatory factors to assist in the treatment of viral FH and other severe inflammatory diseases.

Conflicts of interest

The authors declare no conflict of interest.

References

- Liu M, Chan CW, McGilvray I, *et al.* Fulminant viral hepatitis: molecular and cellular basis, and clinical implications. *Expert Rev Mol Med*, 2001, 2001: 1–19.
- Marsden PA, Ning Q, Fung LS, *et al.* The Fgl2/fibroleukin prothrombinase contributes to immunologically mediated thrombosis in experimental and human viral hepatitis. *J Clin Invest*, 2003, 112: 58–66.
- Sarin SK, Kumar A, Almeida JA, *et al.* Acute-on-chronic liver failure: consensus recommendations of the Asian Pacific Association for the study of the liver (APASL). *Hepatology*, 2009, 3: 269–282.
- McGuire VA, Arthur JS. Subverting Toll-like receptor signaling by bacterial pathogens. *Front Immunol*, 2015, 6: 607.
- Chow J, Franz KM, Kagan JC. PRRs are watching you: Localization of innate sensing and signaling regulators. *Virology*, 2015, 0: 104–109.
- O'Neill LA, Bowie AG. The family of five: TIR-domain-containing adaptors in Toll-like receptor signalling. *Nat Rev Immunol*, 2007, 7: 353–364.
- Johansson C, Wetzel JD, He JP, *et al.* Type I interferons produced by hematopoietic cells protect mice against lethal infection by mammalian reovirus. *J Exp Med*, 2007, 204: 1349–1358.
- Madera RF, Libraty DH. The role of MyD88 signaling in heterosubtypic influenza A virus infections. *Virus Res*, 2013, 171: 216–221.
- Seo SU, Kwon HJ, Song JH, *et al.* MyD88 signaling is indispensable for primary influenza A virus infection but dispensable for secondary infection. *J Virol*, 2010, 84: 12713–12722.
- Rudd BD, Schaller MA, Smit JJ, *et al.* MyD88-mediated instructive signals in dendritic cells regulate pulmonary immune responses during respiratory virus infection. *J Immunol*, 2007, 178: 5820–5827.
- Phipps S, Lam CE, Mahalingam S, *et al.* Eosinophils contribute to innate antiviral immunity and promote clearance of respiratory syncytial virus. *Blood*, 2007, 110: 1578–1586.
- Zhou SH, Kurt-Jones EA, Mandell L, *et al.* MyD88 is critical for the development of innate and adaptive immunity during acute lymphocytic choriomeningitis virus infection. *Eur J Immunol*, 2010, 35: 822–830.
- Lang KS, Navarini AA, Recher M, *et al.* MyD88 protects from lethal encephalitis during infection with vesicular stomatitis virus. *Eur J Immunol*, 2010, 37: 2434–2440.
- Vénéreau E, Ceriotti C, Bianchi ME. DAMPs from cell death to new life. *Frontiers Immunol*, 2015, 6: 422.
- Andersson U, Tracey KJ. HMGB1 is a therapeutic target for sterile inflammation and infection. *Annu Rev Immunol*, 2011, 29: 139–162.
- Scaffidi P, Misteli T, Bianchi ME. Release of chromatin protein HMGB1 by necrotic cells triggers inflammation. *Nature*, 2002, 418: 191–195.
- Pandolfi F, Altamura S, Frosali S, *et al.* Key role of DAMP in inflammation, cancer, and tissue repair. *Clin Ther*, 2016, 38: 1017–1028.
- Duan E, Wang D, Luo R, *et al.* Porcine reproductive and respiratory syndrome virus infection triggers HMGB1 release to promote inflammatory cytokine production. *Virology*, 2014, 468–470: 1–9.
- Fraisier C, Papa A, Almeras L. High-mobility group box-1, promising serological biomarker for the distinction of human WNV disease severity. *Virus Res*, 2015, 195: 9–12.
- Yu R, Yang DR, Lei SH, *et al.* HMGB1 promotes hepatitis C virus replication by interaction with stem-loop 4 in the viral 5' untranslated region. *J Virol*, 2016, 90: 2332–2344.
- Moisy D, Avilov SV, Jacob Y, *et al.* HMGB1 protein binds to influenza virus nucleoprotein and promotes viral replication. *J Virol*, 2012, 86: 9122–9133.
- Yamamoto M, Sato S, Hemmi H, *et al.* Role of adapter TRIF in the MyD88-independent toll-like receptor signaling pathway. *Science*, 2003, 301: 640–643.
- Godfraind C, Langreth SG, Cardellicchio CB, *et al.* Tissue and cellular distribution of an adhesion molecule in the carcinoembryonic antigen family that serves as a receptor for mouse hepatitis virus. *Lab Invest*, 1995, 73: 615–627.
- Liu JJ, Tan YL, Zhang JY, *et al.* C5aR, TNF- α , and FGL2 contribute to coagulation and complement activation in virus-induced fulminant hepatitis. *J Hepatology*, 2015, 62: 354–362.
- Xu GL, Chen J, Yang F, *et al.* C5a/C5aR pathway is essential for the pathogenesis of murine viral fulminant hepatitis by way of potentiating Fgl2/fibroleukin expression. *Hepatology*, 2014, 60: 114–124.
- Guo S, Yang CY, Diao B, *et al.* The NLRP3 inflammasome and IL-1 β accelerate immunologically mediated pathology in experimental viral fulminant hepatitis. *PLoS Pathog*, 2015, 11: e1005216.
- Sonnenberg GF, Artis D. Innate lymphoid cells in the initiation, regulation and resolution of inflammation. *Nat Med*, 2015, 21: 698–708.
- McKenzie ANJ, Spits H, Eberl G. Innate lymphoid cells in inflammation and immunity. *Immunity*, 2014, 41: 366–374.
- Ibrahim, Z.A., *et al.*, RAGE and TLRs: Relatives, friends or neighbours? *Molecular Immunology*, 2013. 56(4): p. 739-744.
- Xie J, Méndez JD, Méndez-Valenzuela V, *et al.* Cellular signalling of the receptor for advanced glycation end products (RAGE). *Cell Signal*, 2013, 25: 2185–2197.
- Shalev I, Wong KM, Foerster K, *et al.* The novel CD4+CD25+ regulatory T cell effector molecule fibrinogen-like protein 2 contributes to the outcome of murine fulminant viral hepatitis. *Hepatology*, 2010, 49: 387–397.
- Parr RL, Fung L, Reneker J, *et al.* Association of mouse fibrinogen-like protein with murine hepatitis virus-induced prothrombinase activity. *J Virol*, 1995, 69: 5033–5038.
- Totura AL, Baric RS. SARS coronavirus pathogenesis: host innate immune responses and viral antagonism of interferon. *Curr Opin Virol*, 2012, 2: 264–275.
- Casanova JL, Abel L, Quintana-Murci L. Human TLRs and IL-1Rs in host defense: natural insights from evolutionary, epidemiological, and clinical genetics. *Ann Rev Immunol*, 2011, 29: 447–491.
- Nash AA, Dutia BM, Stewart JP, *et al.* Natural history of murine γ -herpesvirus infection. *Philos Trans R Soc Lond B Biol Sci*, 2001, 356: 569–579.
- Eberl G, Colonna M, Di Santo JP, *et al.* Innate lymphoid cells. Innate lymphoid cells: a new paradigm in immunology. *Science*, 2015, 348: aaa6566.
- Goldberg R, Prescott N, Lord GM, *et al.* The unusual suspects--innate lymphoid cells as novel therapeutic targets in IBD. *Nat Rev Gastroenterol Hepatol*, 2015, 12: 271–283.
- Xu H, Wang X, Lackner AA, *et al.* Type 3 innate lymphoid cell depletion is mediated by TLRs in lymphoid tissues of simian immunodeficiency virus-infected macaques. *FASEB J*, 2015, 29: 5072–5080.
- Monticelli LA, Sonnenberg GF, Abt MC, *et al.* Innate lymphoid cells promote lung-tissue homeostasis after infection with influenza virus. *Nat Immunol*, 2011, 12: 1045–1054.

40. Yang C, Chen Y, Guo G, *et al.* Expression of B and T lymphocyte attenuator (BTLA) in macrophages contributes to the fulminant hepatitis caused by murine hepatitis virus strain-3. *Gut*, 2013, 62: 1204–1213.
41. Phillipson M, Kubes P. The neutrophil in vascular inflammation. *Nat Med*, 2010, 17: 1381–1390.
42. Bianchi ME. HMGB1 loves company. *J Leukoc Biol*, 2009, 86: 573–576.
43. Borde C, Barnay-Verdier S, Gaillard C, *et al.* Stepwise release of biologically active HMGB1 during HSV-2 infection. *PLoS One*, 2011, 6: e16145.
44. Chen LC, Yeh TM, Wu HN, *et al.* Dengue virus infection induces passive release of high mobility group box 1 protein by epithelial cells. *J Infect*, 2008, 56: 143–150.

DOI 10.1007/s10330-018-0329-9

Cite this article as: Deng JZ, Ning Q, Yan WM, *et al.* *MyD88* exacerbates immunological pathology in experimental viral fulminant hepatitis. *Oncol Transl Med*, 2019, 5: 58–67.